

ANGULAR CORRELATIONS BETWEEN THE CHARGED PARTICLES PRODUCED IN pp COLLISIONS AT ISR ENERGIES

K EGGERT, H FRENZEL and W THOMÉ

III Physikalisches Institut der Technischen Hochschule, Aachen, Germany

B BETEV *, P DARRIULAT, P DITTMANN,
M HOLDER, K T McDONALD, T MODIS and H G. PUGH **
CERN, Geneva, Switzerland

K TITTEL

Institut für Hochenergiephysik, Heidelberg, Germany

I. DERADO, V ECKARDT, H J GEBAUER,
R MEINKE, O R SANDER *** and P SEYBOTH
Max-Planck-Institut für Physik und Astrophysik, Munich, Germany

Received 11 November 1974

Abstract We present an analysis of rapidity and azimuthal correlations between the charged products of pp collisions at ISR energies. The use of streamer chambers as detectors permits a study of the correlation mechanism at fixed multiplicities. The analysis is restricted to the central rapidity region to suppress diffractive production. A strong short-range correlation is observed, which can be described by independent emission of low-multiplicity clusters, suggestive of abundant resonance production.

1 Introduction

The existence of short-range rapidity correlation among the products of pp collisions at ISR energies is well established [1]. However, many different processes may generate rapidity correlations, and care must be exercised in interpreting the data. A well-known example is the coexistence of diffraction and pionization components. In addition to the genuine correlations characteristic of each mechanism, the correlation function contains a cross term which merely reflects the twofold nature of

* On leave from Institute of Nuclear Research, Sofia, Bulgaria

** On leave from University of Maryland, College Park, Md, USA

*** Now at Lawrence Berkeley Laboratory, Berkeley, Cal, USA

the production process. It is therefore important to restrict correlation studies to events of a single kind, as far as possible. We limit the present analysis to events with a large number of particles in the central region. At ISR energies, where the rapidity plateau has become wider, this is an efficient way of selecting non-diffractive processes. It implies, however, that correlations with a range larger than the rapidity interval of the analysis will not be detected.

Another difficulty in correlation analyses is the mixing of events with different numbers of particles*. Averaging over multiplicities inextricably mixes the properties of the correlation mechanism with those of the multiplicity distribution. Instead, the study of correlations at fixed multiplicities allows one to separate both effects and to investigate the behaviour of the correlation function as a function of multiplicity.

The measurements reported here were performed with two large streamer chambers surrounding an intersection region of the CERN ISR. There was no magnetic field, only angular variables were measured. In addition to a straightforward measurement of the charged particle multiplicity, such a detector provides good rejection of charged secondaries not pointing to the production vertex.

After a brief description of the detector and of the main features of data reduction, we present an analysis of two-particle rapidity correlations at centre-of-mass energies of 23 and 53 GeV. We then study correlations as a function of azimuth and rapidity, and conclude with a brief comment on three-particle correlations.

2. Apparatus

An intersection region of the ISR is surrounded by two double-gap streamer chambers above and below the beam pipes (fig. 1). Apart from the 8 cm gap between the chambers, they cover the full solid angle. Each chamber is 50 cm high, 270 cm long (along the beams), and 125 cm wide (transverse to the beams). The geometry of the sensitive volumes is such that the maximum visible track length is 30 cm in the forward direction and 13 cm on the sides. The dependence of the acceptance upon production angle is governed by the effect of the gap between the chambers. Over most of the angular range it remains equal to 86% but falls steeply in the forward direction to zero below 40 mrad. The tracks are photographed through two 8° stereo views recorded on a single 35 mm film.

The apparatus is triggered by a coincidence between large scintillator hodoscopes on each downstream side of the interaction region. This trigger observes a cross section of 34 mb (36 mb) at $\sqrt{s} = 23$ GeV (53 GeV), of which less than 6 mb (4 mb) are from elastic scattering. About 4.3 mb (2.8 mb) of the interactions which fail to trigger the detector would have had tracks in the streamer chambers, but only 2.3 mb (1.2 mb) are associated with events of the type selected in the present analysis.

* There exists an abundant literature on correlations. The point of view adopted here is developed in Morel and Plaut [2], which also contains extensive references.

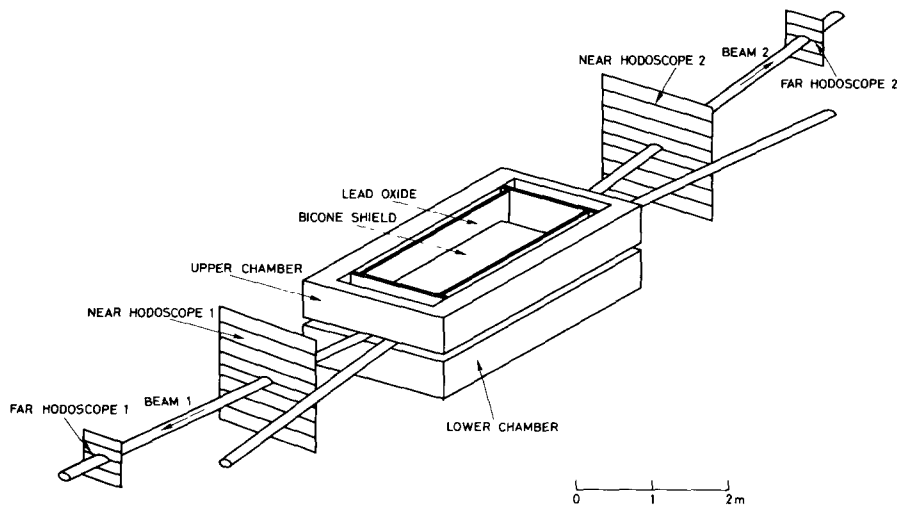


Fig 1 Schematic layout of the apparatus Optical system and HV generators have been omitted for clarity.

3. Data reduction

Events are scanned and measured on image plane digitizing projectors. Six percent of the pictures are rejected for a bad high-voltage pulse, two percent for a second event detected by the electronics during the sensitive time ($1 \mu\text{sec}$) of the streamer chambers, and eight percent for a large number of background tracks not associated with the interaction. About 22% (9%) of triggers at 23 GeV (53 GeV) show no track in the streamer chambers. Three points are measured in each view on all tracks which point into the vicinity of the interaction region. The setting error is about 12μ on film (2 mm in space).

Tracks are reconstructed as straight lines in space using the two stereo views. Typical uncertainties of the track extrapolation to the interaction region are 0.6 cm (8 cm) in the horizontal (vertical) projection. The interaction point is found by an iterative least squares fit to the measured tracks. The resulting errors on the final vertex position are about 0.3 cm in the horizontal plane and 4 cm along the vertical direction. All tracks pointing to the vertex within 3 standard deviations are accepted, and their directions in space are recalculated using the interaction vertex as an additional constraint. In this last step, the vertex is assumed to lie in the plane of the beams, as the heights of the beams are much smaller than vertical reconstruction uncertainties, and their positions are accurately known.

In the absence of momentum measurement and particle identification, each track is completely described by its azimuth ϕ and production angle θ . These quantities are calculated in the lab system and transformed to the centre-of-mass system under the assumption that the produced particles have zero mass. Because of the small

crossing angle (15°) of the beams this approximation has no important effect on our analysis. We also use the quantity $\eta = -\log \tan(\frac{1}{2}\theta)$, referred to as “rapidity” whenever the distinction between it and the true rapidity is irrelevant to our purpose. Typical uncertainties due to reconstruction errors are 5° in ϕ and 0.1 unit in η .

From a Monte-Carlo simulation reproducing inclusive momentum distributions and event multiplicities, we estimate a contamination of 3% in the central region due to converted γ rays, Dalitz pairs, and secondaries of nuclear interactions. The K^0 production is estimated to contribute less than 8% of the charged particles accepted by our selection criteria.

We report here on a small fraction of the pictures recorded, namely 3050 events at $\sqrt{s} = 23$ GeV and 2408 events at $\sqrt{s} = 53$ GeV, corresponding to 1022 and 1462 events, respectively, for the restricted samples used in the analysis.

4. Two-particle rapidity correlations

Before presenting and discussing the rapidity correlations observed in the data, we briefly introduce the formalism used.

In a rapidity interval $|\eta| \leq \eta_{\max}$ we define

- (a) the number of charged particles, n ,
- (b) the charged particle density

$$\rho_n^I(\eta) = \frac{1}{n\sigma_n} \frac{d\sigma_n}{d\eta},$$

- (c) the charged pair density

$$\rho_n^{II}(\eta_1, \eta_2) = \frac{1}{n(n-1)\sigma_n} \frac{d^2\sigma_n}{d\eta_1 d\eta_2},$$

- (d) the correlation function

$$C_n^{II}(\eta_1, \eta_2) = \rho_n^{II}(\eta_1, \eta_2) - \rho_n^I(\eta_1) \rho_n^I(\eta_2), \quad (1)$$

with $d\sigma_n/d\eta$ = differential cross section for producing a charged particle at rapidity η when n charged particles are produced between $-\eta_{\max}$ and $+\eta_{\max}$. The above quantities obey the normalization relations

$$n\sigma_n = \int_{-\eta_{\max}}^{+\eta_{\max}} \frac{d\sigma_n}{d\eta} d\eta, \quad \int_{-\eta_{\max}}^{+\eta_{\max}} \rho_n^I(\eta) d\eta = 1,$$

$$\int_{-\eta_{\max}}^{+\eta_{\max}} \int_{-\eta_{\max}}^{+\eta_{\max}} \rho_n^{II}(\eta_1, \eta_2) d\eta_1 d\eta_2 = 1, \quad \int_{-\eta_{\max}}^{+\eta_{\max}} \int_{-\eta_{\max}}^{+\eta_{\max}} C_n^{II}(\eta_1, \eta_2) d\eta_1 d\eta_2 = 0.$$

In the absence of correlation, C_n^{II} is zero everywhere by definition

These definitions differ from those usually adopted but lead to relations which are simpler and have a more transparent interpretation In particular, in the case of independent cluster emission [2], C_n^{II} takes the simple form

$$C_n^{\text{II}}(\eta_1, \eta_2) = \alpha_n^{\text{II}} [\Gamma_n^{\text{II}}(\eta_1, \eta_2) - \rho_n^{\text{I}}(\eta_1) \rho_n^{\text{I}}(\eta_2)], \quad (2)$$

where α_n^{II} is the relative number of pairs with both particles in the same cluster and $\Gamma_n^{\text{II}}(\eta_1, \eta_2)$ is the two-particle rapidity density (with unit integral in the domain $|\eta| < \eta_{\text{max}}$) for particles in the same cluster Namely, defining K as the charged multiplicity of a cluster and averaging over clusters,

$$\alpha_n^{\text{II}} = \frac{n}{\langle K \rangle} \frac{\langle K(K-1) \rangle}{n(n-1)} = \frac{1}{n-1} \frac{\langle K(K-1) \rangle}{\langle K \rangle}$$

Whenever a short-range component dominates, relation (2) provides an elegant parametrization of the correlation function It is only in this case, in which Γ_n^{II} vanishes at large $|\eta_1 - \eta_2|$, that relation (2) gives an unambiguous determination of

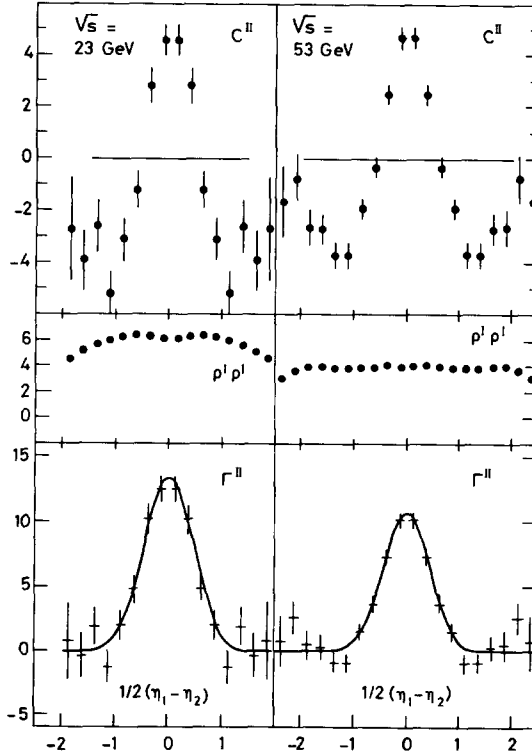


Fig 2 The functions C^{II} , $\rho^{\text{I}}\rho^{\text{I}}$, and Γ^{II} , in units of 10^{-2} versus $\frac{1}{2}(\eta_1 - \eta_2)$ Normalizations are in the square $|\eta| < 2(2.5)$ at $\sqrt{s} = 23(53)$ GeV Γ^{II} is determined from a fit with parameters listed in table 1 The pair densities are symmetrized as $\frac{1}{2}[\rho^{\text{II}}(\eta_1 - \eta_2) + \rho^{\text{II}}(\eta_2 - \eta_1)]$

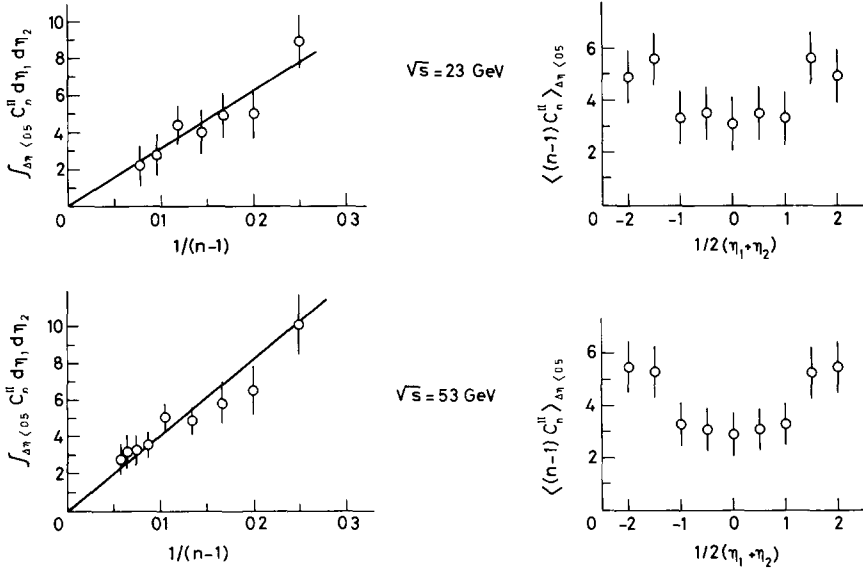


Fig 3 Left the dependence of C_n^{II} (integrated over the region $\Delta\eta < 0.5$) upon $1/(n-1)$ Right the dependence of C_n^{II} (integrated over the region $\Delta\eta < 0.5$) upon $\frac{1}{2}(\eta_1 + \eta_2)$

α_n^{II} and Γ_n^{II} Without any specific assumption it gives a measure of the strength and range of the correlation function through α_n^{II} and Γ_n^{II} . While the most naive cluster models would assume that $(n-1)\alpha_n^{\text{II}}$ and Γ_n^{II} are multiplicity independent, they need not be so.

We have calculated the correlation functions $C_n^{\text{II}}(\eta_1, \eta_2)$ at both beam energies. In each case they show a structure characteristic of short-range rapidity correlation (fig 2). In addition, they exhibit a feature which greatly simplifies their study, namely that, within errors, $(n-1)C_n^{\text{II}}$ depends neither on n nor on $\eta_1 + \eta_2$ but only on $\eta_1 - \eta_2$.

To illustrate the absence of n dependence we integrate C_n^{II} over a domain of strong positive correlation taken as $|\eta_1 - \eta_2| \leq 0.5$ and study the variation with n of the integral. Similarly we study the $\eta_1 + \eta_2$ dependence of $(n-1)C_n^{\text{II}}$ in the interval $|\eta_1 - \eta_2| \leq 0.5$ after having averaged this quantity over n . We find that within errors $(n-1)C_n^{\text{II}}$ does not depend upon n and depends only weakly upon $\eta_1 + \eta_2$ when n and η are limited to the range $6 \leq n \leq 15$ ($6 \leq n \leq 20$) and $|\eta| \leq 2$ ($|\eta| \leq 2.5$) in the 23 GeV (53 GeV) data (fig 3).

We now concentrate on the dependence of

$$C^{\text{II}}(\eta_1 - \eta_2) = \langle (n-1)C_n^{\text{II}}(\eta_1, \eta_2) \rangle$$

upon the single variable $\eta_1 - \eta_2$, where the average over n is performed in the multiplicity intervals previously mentioned.

Table 1
Two-particle rapidity correlation

$$\langle (n-1)C_n^{\text{II}} \rangle \equiv C^{\text{II}}(\eta_1, \eta_2) = \alpha^{\text{II}} [\Gamma^{\text{II}}(\eta_1, \eta_2) - \rho^{\text{I}} \rho^{\text{I}}(\eta_1, \eta_2)],$$

$$\Gamma^{\text{II}}(\eta_1, \eta_2) \propto \exp \left\{ - \frac{(\eta_1 - \eta_2)^2}{4\delta^2} \right\}$$

\sqrt{s}	23 GeV		53 GeV	
Selected rapidity window	$ \eta \leq 2.0$		$ \eta \leq 2.5$	
Mean multiplicity in selected rapidity window	5.8		8.9	
Selected multiplicity range in rapidity window	$6 \leq n \leq 15$		$6 \leq n \leq 20$	
Number of selected events	1022		1462	
	Strength α^{II}	Range δ	Strength α^{II}	Range δ
Raw data	0.72 ± 0.07	0.62 ± 0.05	0.76 ± 0.04	0.59 ± 0.03
Acceptance correction	$+0.15 \pm 0.05$	0 ± 0.03	$+0.15 \pm 0.05$	0 ± 0.03
Edge-effect correction	$+0.25 \pm 0.10$	$+0.06 \pm 0.03$	$+0.20 \pm 0.10$	$+0.03 \pm 0.02$
Zero mass approximation	$+0.10 \pm 0.10$	0 ± 0.05	$+0.10 \pm 0.10$	0 ± 0.05
Hypothesis of n and $\eta_1 + \eta_2$ independence	0 ± 0.05		0 ± 0.05	
Raw data $n \leq 9$	0.71 ± 0.08	0.61 ± 0.06	0.74 ± 0.05	0.60 ± 0.04
Raw data $n > 9$	0.70 ± 0.16	0.65 ± 0.12	0.82 ± 0.06	0.56 ± 0.04
All corrections included	1.22 ± 0.17	0.68 ± 0.08	1.21 ± 0.16	0.62 ± 0.07

The functions $C^{\text{II}}(\eta_1 - \eta_2)$ and

$$\rho^{\text{I}} \rho^{\text{I}}(\eta_1 - \eta_2) = \langle \rho_n^{\text{I}}(\eta_1) \rho_n^{\text{I}}(\eta_2) \rangle$$

are displayed in fig 2. Their dependence upon $\eta_1 - \eta_2$ suggests that we may assign all the correlations to a short-range effect which we parametrize as a Gaussian

$$\Gamma^{\text{II}}(\eta_1, \eta_2) \propto \exp \left[- \frac{(\eta_1 - \eta_2)^2}{4\delta^2} \right].$$

This specific form would be obtained for clusters decaying into uncorrelated particles, with a Gaussian single-particle rapidity distribution of variance δ . Good fits to the form

$$C^{\text{II}}(\eta_1, \eta_2) = \alpha^{\text{II}} [\Gamma^{\text{II}}(\eta_1, \eta_2) - \rho^{\text{I}}\rho^{\text{I}}(\eta_1, \eta_2)]$$

are obtained (fig 2) The results are listed in table 1, together with various corrections and contributions to the uncertainties, as discussed below

(a) Raw data We have rejected narrow pairs (opening angle $< 1.8^\circ$) corresponding to γ rays converted in the vacuum chamber and to Dalitz pairs Including these narrow pairs would increase the correlation strength α^{II} by 0.06

Statistical errors are calculated with Poisson statistics, but the contributions of ρ^{II} and $\rho^{\text{I}}\rho^{\text{I}}$ are treated independently. We have checked that this does not introduce appreciable biases.

(b) Acceptance correction. This is estimated from an analysis of the actual data, after having removed more tracks, according to the known rapidity dependence of the acceptance of the detector A particle in a correlated pair is occasionally missed, but this depends little upon the rapidity width of the pair the strength of the correlation appears smaller but its range is virtually unaffected.

(c) Edge effects. Correlated pairs with only one particle inside the rapidity window do not contribute to the positive correlation The restriction of the analysis to a narrow rapidity interval, and the choice of a Gaussian form for Γ^{II} , filter out long-range components from the correlation function with a cut-off depending upon the ratio δ/η_{max} The correction is made with a Monte-Carlo calculation in which all particles are produced in Gaussian pairs with $\delta = 0.65$

(d) Zero mass approximation A pair of particles with masses m and invariant mass M has a rapidity difference limited to $\Delta y \leq \arcsin h [(M^2/2m^2) - 1]$ There is no such bound when the pseudorapidity $\eta = -\log \tan \frac{1}{2}\theta$ is used instead This introduces long tails in the two-particle density and causes an effective decrease of the correlation strength α^{II} . The correction in table 1 was estimated from a model calculation with ρ and ω resonances

(e) Hypothesis of independence over n and $\eta_1 + \eta_2$ We have checked that the results were not significantly modified when the multiplicity range was split into two intervals (table 1) nor when the fit was made in η_1 and η_2 explicitly, rather than in $\eta_1 - \eta_2$ We also checked that the results were not substantially affected by a change of ± 0.5 unit in η_{max} .

(f) We have also estimated the contribution to C^{II} of different rapidity distributions between particles of different types This induces an apparent correlation which, in the case of π^+ and π^- , takes the form

$$\delta C^{\text{II}} \simeq \frac{1}{4} (\rho_+^{\text{I}} - \rho_-^{\text{I}})_{\eta_1} (\rho_+^{\text{I}} - \rho_-^{\text{I}})_{\eta_2}$$

From published ISR data [3] we find that δC^{II} never exceeds 0.003

The results of this analysis indicate that

(i) Within errors, there is no s dependence of the correlation mechanism

(ii) The range δ of the correlation function is of the order of 0.65 rapidity units. For a pair of pions with 300 MeV/c transverse momenta, it corresponds to an average invariant mass between 480 and 710 MeV/c², depending upon the azimuthal opening of the pair

(iii) The strength of the correlation and its multiplicity dependence are consistent with independent emission of low multiplicity clusters. Using a single fit for the multiplicity range considered, we found

$$\alpha^{\text{II}} = \frac{\langle K(K-1) \rangle}{\langle K \rangle} = \langle K \rangle - 1 + \frac{\langle K^2 \rangle - \langle K \rangle^2}{\langle K \rangle} = 1.2 \pm 0.2,$$

which implies an average charge multiplicity per cluster

$$\langle K \rangle \leq 2.2 \pm 0.2$$

5 Azimuthal correlations

In the previous section no reference was made to a possible azimuthal dependence of the correlation. In complete analogy with relation (1) we may define a two-particle azimuthal correlation function

$$C_n^{\text{II}}(\phi_1, \phi_2) = \rho_n^{\text{II}}(\phi_1, \phi_2) - \rho_n^{\text{I}}(\phi_1) \rho_n^{\text{I}}(\phi_2) \tag{3}$$

Here again we only consider events with n charged particles in the rapidity interval $|\eta| \leq \eta_{\text{max}}$. The independence of $C_n^{\text{II}}(\phi_1, \phi_2)$ upon $\phi_1 + \phi_2$ is now a simple consequence of rotational invariance. As in the previous section, we find that $(n-1) C_n^{\text{II}}(\phi_1, \phi_2)$ does not depend upon n within errors. This permits us to define

$$C^{\text{II}}(\Delta\phi) = \langle (n-1) C_n^{\text{II}}(\phi_1, \phi_2) \rangle,$$

which only depends upon $\Delta\phi = |\phi_1 - \phi_2|$ and is displayed in fig. 4 for both sets of data. It shows an excess of pairs with large $\Delta\phi$. This can be simply measured in terms of the asymmetry parameter

$$A_n = \left(\int_{\frac{1}{2}\pi}^{\pi} \rho_n^{\text{II}} d\Delta\phi - \int_0^{\frac{1}{2}\pi} \rho_n^{\text{II}} d\Delta\phi \right) \left(\int_0^{\pi} \rho_n^{\text{II}} d\Delta\phi \right)^{-1}$$

We find $(n-1) A_n = 0.30 \pm 0.06$ (0.25 ± 0.04) at $\sqrt{s} = 23$ GeV (53 GeV).

To investigate the relation between rapidity and azimuthal correlations, we describe them simultaneously with a single angular correlation function defined in the four-dimensional space $(\eta_1, \eta_2, \phi_1, \phi_2)$. The generalization of relations (1) and (3) is straightforward

$$C_n^{\text{II}}(\eta_1, \phi_1, \eta_2, \phi_2) = \rho_n^{\text{II}}(\eta_1, \phi_1, \eta_2, \phi_2) - \rho_n^{\text{I}}(\eta_1, \phi_1) \rho_n^{\text{I}}(\eta_2, \phi_2), \tag{4}$$

where the density functions are normalized to one in the four-dimensional volume

$$|\eta_{1,2}| \leq \eta_{\text{max}}, \quad 0 \leq \phi_{1,2} \leq 2\pi$$

After averaging over $\eta_1 + \eta_2, \phi_1 + \phi_2$, and n , we obtain an angular correlation function

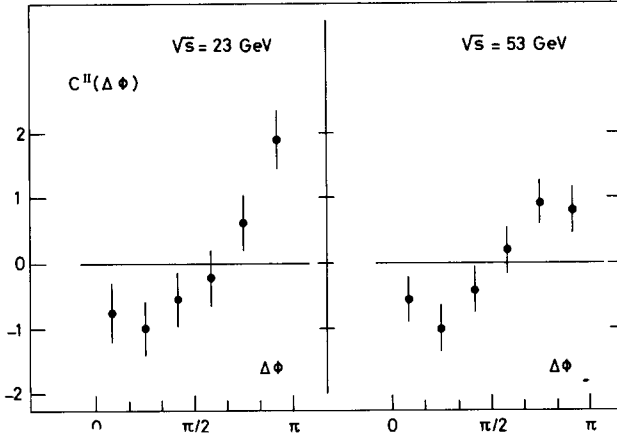


Fig 4 The measured azimuthal correlation functions, $C^{\text{II}}(\Delta\phi)$, in units of 10^{-2}

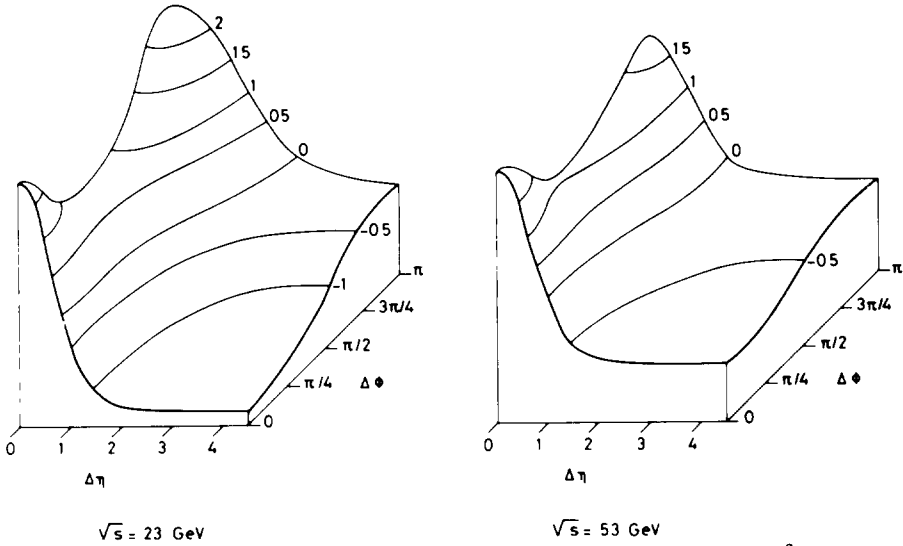


Fig 5 The measured angular correlation functions, $C^{\text{II}}(\Delta\eta, \Delta\phi)$, in units of 10^{-3} For clarity, smooth curves have been drawn through the data which have typical error bars of $\pm 0.4 \times 10^{-3}$

$$C^{\text{II}}(\Delta\eta, \Delta\phi) = \langle (n - 1) C_n^{\text{II}}(\eta_1, \phi_1, \eta_2, \phi_2) \rangle ,$$

which only depends upon $\Delta\eta = |\eta_1 - \eta_2|$ and $\Delta\phi$, and is displayed in fig 5 for both sets of data A rather complex structure emerges, with the following properties

- (i) The short-range rapidity correlation persists over the full $\Delta\phi$ range
- (ii) The range of the rapidity correlation is larger towards $\Delta\phi = \pi$ than towards $\Delta\phi = 0$ We find at $\sqrt{s} = 23 \text{ GeV}$ (53 GeV)

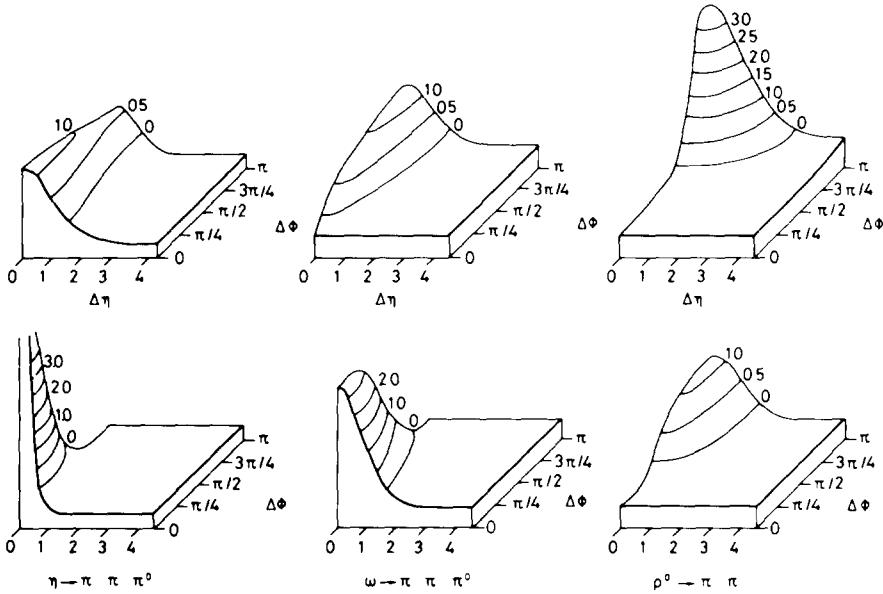


Fig. 6. Calculated angular correlation functions, $C^{II}(\Delta\eta, \Delta\phi)$, for $\rho^0 \rightarrow \pi^+\pi^-$, η and $\omega \rightarrow \pi^+\pi^-\pi^0$ decays. Invariant cross sections for meson production have the form $\exp(-\frac{1}{4}y^2) \times \exp(-Bp_T)$, where y and p_T are the rapidity and transverse momentum of the decaying meson B has the value 6 GeV^{-1} in the case of the top curves. For the bottom curves, B was adjusted to yield an invariant cross section of the form $\exp(-6p_T)$ for the decay pions. Density functions are normalized in the square $|\eta| < 2.5$ as for the $\sqrt{s} = 53 \text{ GeV}$ data. Lines of constant $C^{II}(\Delta\eta, \Delta\phi)$ are labelled in units of 10^{-3} .

$$\begin{aligned} \delta &= 0.54 \pm 0.04 \quad (0.49 \pm 0.02) & \text{for } \Delta\phi < \frac{1}{2}\pi, \\ \delta &= 0.89 \pm 0.05 \quad (0.86 \pm 0.04) & \text{for } \Delta\phi > \frac{1}{2}\pi \end{aligned}$$

It is instructive to compare these data with angular correlations generated by independent emission of low-mass resonances. For this we have calculated the effect of three typical decays, $\rho \rightarrow \pi^+\pi^-$, $\omega \rightarrow \pi^+\pi^-\pi^0$, and $\eta \rightarrow \pi^+\pi^-\pi^0$. The results, displayed in fig. 6, have the following properties

(a) The ρ mesons induce rapidity correlations towards $\Delta\phi = \pi$ only, while η and ω mesons do so over the full $\Delta\phi$ range. Any two-body decay with a Q value large in comparison with the transverse momentum of the parent, would qualitatively behave as ρ mesons.

(b) The ranges of the rapidity correlations vary little with $\Delta\phi$. They are of the order of 0.8, 0.6, and 0.5 for ρ , ω , and η , respectively. The differences are due to the different average invariant masses of the $\pi^+\pi^-$ pair in the three decays.

(c) The strength of the short-range part of the rapidity correlation varies with $\Delta\phi$ in a way that depends only very little upon the rapidity distribution but very

much upon the transverse momentum (p_T) distribution adopted for the decaying meson. This is illustrated in fig. 6 where two extreme forms were taken for the invariant production cross sections: one with $\exp(-6p_T)$ for the resonances themselves (upper curves) and the other such that the decay pions obey $\exp(-6p_T)$ (lower curves). While the domain of positive correlation for ρ mesons is concentrated towards $\Delta\phi = \pi$ in both cases, it shifts from large $\Delta\phi$ to small $\Delta\phi$ for ω and η mesons. In general, when the transverse momentum becomes large compared to the Q value of the decay, positive correlations become significant in the vicinity of $\Delta\phi = 0$.

It is noteworthy that combined production of ρ^0 , ω and η mesons is able to describe most of the qualitative properties of the angular correlation functions*. In particular, the $\Delta\phi$ dependence of the rapidity correlation range is well reproduced.

6. Three-particle correlations

In an independent cluster emission model where there are only two-particle correlations, the ratio between correlated pairs and single-particle production is simply related to α_n^{II} . This is no longer true in the presence of correlations of higher order. Such correlations could arise, for example, from the production of narrow clusters with more than two charged particles, or from possible medium-range correlations between charged pairs. To see if multiplets other than pairs are produced, we now study three-particle correlations.

In complete analogy with relation (1) we define a three-particle correlation function

$$C_n^{\text{III}}(\eta_1, \eta_2, \eta_3) = \rho_n^{\text{III}}(\eta_1, \eta_2, \eta_3) - \tilde{\rho}_n^{\text{III}}(\eta_1, \eta_2, \eta_3), \quad (5)$$

where ρ_n^{III} is the observed three-particle density and $\tilde{\rho}_n^{\text{III}}$ the three-particle density in the absence of three-particle correlation

$$\begin{aligned} \tilde{\rho}_n^{\text{III}} &= \rho_n^{\text{II}}(\eta_1, \eta_2) \rho_n^{\text{I}}(\eta_3) + \rho_n^{\text{II}}(\eta_2, \eta_3) \rho_n^{\text{I}}(\eta_1) + \rho_n^{\text{II}}(\eta_3, \eta_1) \rho_n^{\text{I}}(\eta_2) \\ &\quad - 2\rho_n^{\text{I}}(\eta_1) \rho_n^{\text{I}}(\eta_2) \rho_n^{\text{I}}(\eta_3). \end{aligned}$$

The three-particle densities are normalized to one in the cube $|\eta_{1,2,3}| \leq \eta_{\text{max}}$.

In analogy with the two-particle case, where structure appears in the $\Delta\eta$ dependence, we define a variable ξ , characteristic of triplet size

$$\xi^2 = (\eta_1 - \eta_2)^2 + (\eta_2 - \eta_3)^2 + (\eta_3 - \eta_1)^2$$

* The decays of ρ^\pm , ω and η mesons produce a higher proportion of charged-neutral pion pairs than of charged-charged ones, thus inducing stronger charged-neutral correlations. We also note that if these mesons are independently produced they generate no correlation between like pions.

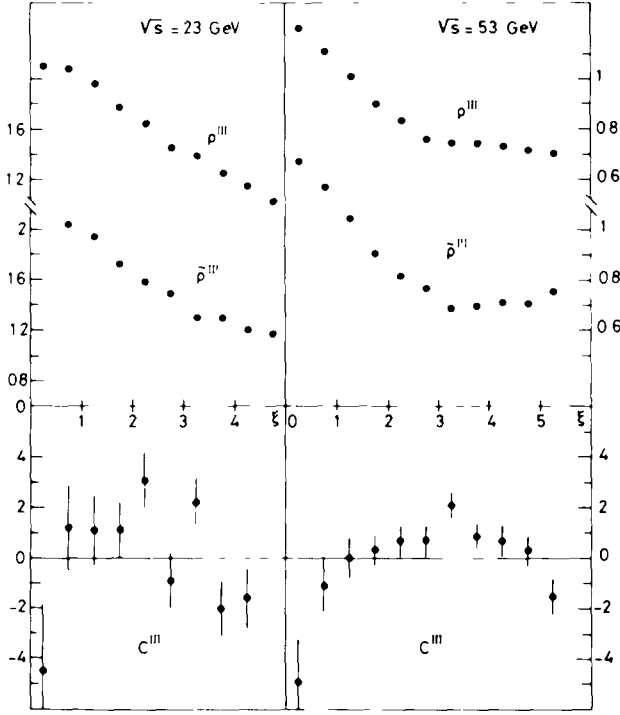


Fig 7 The three-particle densities ρ^{III} and $\tilde{\rho}^{\text{III}}$, and the three-particle correlation function C^{III} , in units for 10^{-2} , versus the triplet size parameter $\xi = \{(\eta_1 - \eta_2)^2 + (\eta_2 - \eta_3)^2 + (\eta_3 - \eta_1)^2\}^{\frac{1}{2}}$

We then average ρ_n^{III} and $\tilde{\rho}_n^{\text{III}}$ over surfaces of constant ξ and define

$$\rho^{\text{III}}(\xi) = \langle \rho_n^{\text{III}}(\xi) \rangle, \quad \tilde{\rho}^{\text{III}}(\xi) = \langle \tilde{\rho}_n^{\text{III}}(\xi) \rangle,$$

where the average over n is performed in the same multiplicity intervals as before. The dependence of ρ^{III} and $\tilde{\rho}^{\text{III}}$ upon ξ is shown in fig 7.

The situation contrasts with the two-particle case where $\rho^{\text{I}}\rho^{\text{I}}(\Delta\eta)$ has no structure and where the presence of correlation is directly visible in $\rho^{\text{II}}(\Delta\eta)$. Here, the density $\tilde{\rho}^{\text{III}}(\Delta\eta)$ is strongly peaked at low ξ values, owing to the short range of the two-particle correlation, and $\rho^{\text{III}}(\xi)$ shows a similar behaviour. In fact, within statistics, $C_n^{\text{III}}(\xi)$ is consistent with zero for all multiplicities.

We can obtain an upper bound on the strength of the three-particle correlation within the framework of the cluster model. We first average $(n-1)(n-2)C_n^{\text{III}}(\xi)$ between $n=6$ and $n=12$, although we have no evidence against a possible n dependence of this expression. We then parametrize

$$C^{\text{III}}(\xi) \equiv \langle (n-1)(n-2)C_n^{\text{III}}(\xi) \rangle = \alpha^{\text{III}} [\Gamma^{\text{III}}(\xi) - \tilde{\Gamma}^{\text{III}}(\xi)], \quad (6)$$

where

$$\alpha^{\text{III}} = \frac{\langle K(K-1)(K-2) \rangle}{\langle K \rangle^3},$$

and $\tilde{\Gamma}^{\text{III}}$ has the same functional dependence upon Γ^{II} and ρ^{I} as $\tilde{\rho}^{\text{III}}$ has upon ρ^{II} and ρ^{I} . This expression emerges from the cluster model, $\Gamma^{\text{III}}(\xi)$ is the three-particle density for particles in the same cluster. We take it to have the form

$$\Gamma^{\text{III}}(\xi) \propto \exp\left(-\frac{\xi^2}{6\delta^2}\right),$$

corresponding to clusters decaying into uncorrelated particles with a Gaussian single-particle distribution of variance δ .

From a common fit to $C^{\text{II}}(\Delta\eta)$ and $C^{\text{III}}(\xi)$ in the $\sqrt{s} = 53$ GeV data, we find

$$\delta = 0.59 \pm 0.07, \quad \alpha^{\text{II}} = 0.76 \pm 0.09, \quad \alpha^{\text{III}} = 0 \begin{matrix} +2 \\ -0 \end{matrix}^5$$

This gives almost no bound on the strength of the three-particle correlation function. If all particles were produced in independent triplets, α^{III} would be 2. To obtain a significant estimate of α^{III} requires a much larger number of events than considered here.

7 Conclusion

Many of the results presented here suggest that an important part of the angular correlations observed in the central region is generated by known resonances.

(i) the dependence upon multiplicity is consistent with independent emission of clusters of less than 2.2 charged particles on the average, at both \sqrt{s} values studied here ($\sqrt{s} = 23$ GeV and $\sqrt{s} = 53$ GeV),

(ii) the range of the rapidity correlation corresponds to that of pairs with low invariant mass,

(iii) we have shown that combined production of η , ω and ρ mesons, as an example, can reproduce qualitatively the observed $\Delta\eta - \Delta\phi$ dependence of the angular correlation function.

These conclusions are supported by observations made at FNAL energies [4], namely the presence of a substantial ρ^0 production in pp and π^-p collisions, and the weakness of correlations between like pions.

In our opinion, lacking detailed knowledge on the production of known meson resonances, it is premature to see evidence for new dynamical processes in angular correlation data.

We thank Professors H. Faissner and N. Schmitz for encouragement and support. We have benefitted from several very instructive discussions with Dr. M. Jacob.

Dr F Schneider and his colleagues have made major contributions to the design and development of the optical system. The success of the experiment has depended upon the excellent technical support of Dr. G Muratori, Messrs H Geissmann, E. Giesche, W Tribanek, H. Utzat and their colleagues. Much help was provided by the ISR staff when installing the experiment at the ISR

We are indebted to H Albrecht, P Allen, G Bohm, K.L Giboni, J Kaltwasser, S Uhlig and G Vesztergombi who have made contributions to the running of the experiment or to its analysis.

The lengthy task of scanning and measuring has been performed with perseverance and care by the scanning teams in the four laboratories.

Partial financial support was given by the Bundesministerium fur Forschung und Technologie.

References

- [1] H Dibon, G Flügge, Ch Gottfried, B M K Nefkens, G Neuhofer, F Niebergall, M Regler, W Schmidt-Parzefal, K R Schubert, P E Schumacher and K Winter, *Phys Letters* 44B (1973) 313,
S R Amendolia, G Belletini, P L Braccini, C Bradaschia, R Castaldi, V Cavasinni, C Cerni, T Del Prete, L Foa, P Giromini, P Laurelli, A Menzione, L Ristori, G Sanguinetti, M Valdata, G Finocchiaro, P Grannis, D Green, R Kephart and R Thun, *Phys Letters* 48B (1974) 359,
L Foa, *Proc 2nd Int Conf on elementary particles, Aix-en-Provence, 1973*, *J de Phys* 34 (1973) C1-317
- [2] A Morel and G Plaut, *Nucl Phys* B78 (1974) 541
- [3] A M Rossi, G Vannini, A Bussiere, E Albini, D D'Alessandro and G Giacomelli, *Nucl Phys* B84 (1975) 269,
M Banner, J L Hamel, J P Pancart, A V Stirling, J Teiger, H Zaccone, J Zsebery, G Bassompierre, M Croissiaux, J Gresser, R Morand, M Riedinger and M Schneegans, *Phys Letters* 41B (1972) 547
- [4] R Singer, Y Cho, T Fields, L G Hyman, P A Schreiner, L Voyvodic, R Walker, J Whitmore, R Engelmann, T Kafka, C Moore and M Pratap, *Phys Letters* 49B (1974) 481, Argonne National Laboratory preprints ANL/HEP 7368 and ANL/HEP 7369, unpublished,
M Pratap, R Engelmann, T Kafka, Y Cho, T H Fields, L G Hyman, R Singer, L Voyvodic, R Walker and J Whitmore, *Phys Rev Letters* 33 (1974) 797,
W T. Ko, Davis preprint UCD-PPI-7-17-74, to appear in the *Proc of the 17th Int Conf on high-energy physics*, London, July 1974
F C Winkelmann, Lawrence Berkeley Laboratory report LBL 3045, presented at the 4th *Int Conf on experimental meson spectroscopy*, Boston, April 1974